$1 ^3A_2$ is not the lowest state, it is unlikely that the T–S transition to $^3A_1$ can gain much intensity from the two low-lying Rydberg transitions to states of symmetry B_2 via spin–orbit coupling.[31] For this reason, it is probable that the interpretation of the observed spectrum as proferred by Judge and Moule is correct. Thus one or both of the two weaker absorption bands, or an as yet undetected band, may be associated with the $^3A_1$ state. The ambiguity may be resolved by explicit evaluation of the spin–orbit interactions and higher level CI calculations, neither of which we are able to do at the present time. Additional experimental work in progress may also resolve the issue.[32]

The next higher triplet state is found to be $^3B_1$ (n′–π*) at 4.96 eV. As the energy of the triplet states are not as well represented

as the energies of the singlet states with the present procedure, it is likely that this state will fall below $^1A_1$ (π–π*). Transition to this state may also borrow intensity from spin–orbit coupling to $^1A_1$ (π–π*) but may be overshadowed by the more intense dipole-allowed transition and thus not be detectable. The remaining low-lying triplet states are Rydberg states and should be close in energy to the corresponding singlet states since exchange integrals between valence and Rydberg orbitals are very small. As can be seen in Figure 2, the states $^3A_1$ (π–π*), $^3B_1$ (n′–π*), and $^3B_2$ (n–5s) decrease in energy as the C=Se bond is stretched while $^3A_2$ (n–π*) and $^3B_2$ (n–5p$_z$) are relatively insensitive.

(31) The spin–orbit part of the total Hamiltonian which causes the mixing of singlet and triplet configurations is a sum of one-electron operators and thus will not significantly mix states which formally differ by more than one spin orbital as do $^3A_1$ (π–π*) and $^1B_2$ (n–5s) or $^1B_2$ (n–5p$_z$).
(32) See footnote 9 of ref 7.

X-ray Analysis of the Effect of Apical Substitution on the Three-Dimensional Features of Isodicyclopentafulvenes. Experimental Demonstration of Minimal Bridgehead C–H Angle Deformation Accompanying Substantial Hybridization Change at the Apical Center[1]

Judith C. Gallucci,* Tina M. Kravetz, Kenneth E. Green, and Leo A. Paquette*

Contribution from the Evans Chemical Laboratories, The Ohio State University, Columbus, Ohio 43210. Received April 1, 1985

Abstract: Single-crystal X-ray analyses have been performed for three isodicyclopentafulvenes. 2-(Diphenylmethylene)-4,5,6,7-tetrahydro-4,7-methano-2*H*-indene (**13**) crystallizes in the monoclinic space group $P2_1/n$ with four molecules in a unit cell of dimensions $a = 9.666$ (5) Å, $b = 17.087$ (7) Å, $c = 11.229$ (6) Å, and $\beta = 116.53$ (4)°. Least-squares refinement resulted in a final conventional R index of 0.070 based on 1671 unique reflections. The exocyclic double bond in this structure is markedly nonplanar. By comparison, 4′,5′,6′,7′-tetrahydro-2′-isopropylidenespiro[cyclopropane-1,2′-[4,7]methano[2*H*]indene] (**14**) crystallizes in the triclinic space group $P\bar{1}$ with unit cell dimensions $a = 9.345$ (2) Å, $b = 10.502$ (2) Å, $c = 5.953$ (1) Å, $\alpha = 91.04$ (1)°, $\beta = 95.46$ (1)°, $\gamma = 84.03$ (1)°, and two molecules per unit cell. Least-squares refinement based on the 1974 unique reflections resulted in a final R index of 0.066. 4,5,6,7-Tetrahydro-2,8-diisopropylidene-4,7-methano-2*H*-indene (**15**) also crystallizes in space group $P\bar{1}$ with two molecules in a unit cell of dimensions $a = 8.078$ (1) Å, $b = 6.341$ (1) Å, $c = 14.003$ (2) Å, $\alpha = 89.38$ (1)°, $\beta = 73.45$ (1)°, and $\gamma = 110.81$ (1)°. Least-squares refinement yielded a final R index of 0.088 for the 1791 unique reflections. The isodicyclopentafulvene core common to all three structures may be described in terms of noncrystallographic mirror symmetry. The angles about the apical methano carbon of the norbornane ring, 96.2°, 96.6°, and 96.7° for **13**, **14**, and **15**, respectively, exhibit the usual deviation from a tetrahedral value. A comparison of the metrical parameters common to these structures results in excellent agreement between **14** and **15**. The somewhat less good agreement in the case of **13** is the likely result of the data set for this structure being the weakest of the three. Since the dihedral angles between the bridgehead C–H bonds and exocyclic π bonds in all three molecules are not significantly different, the increased tendency of isodicyclopentadiene congeners **10** and **12** to enter into Diels–Alder reaction from above-plane cannot find its origin in a perturbation of torsional strain effects either in the cycloaddition transition states or in the products. Rather, the modulation of stereoselectivity is satisfactorily accommodated within the guidelines of the Paquette–Gleiter theory.

Proper fusion to a 1,3-butadiene unit of a structural component unsymmetrical about the π-plane permits, in principle, the onset of π-facial discrimination.[2] Stereoselectivity of this type, which can provide valuable insight into reaction mechanism, has only recently been given serious attention.[3] The primary focus of this effort has been the isodicyclopentadiene system **1**.[2,4–6] Detailed

1

analysis of **1** by various semiempirical methods has pointed to substantive admixing of properly symmetric high-lying σ orbitals

(1) Electronic Control of Stereoselectivity. 30. For Part 29, see: Paquette, L. A.; Hathaway, S. J., *J. Am.* Chem. *Soc.*, submitted.
(2) Paquette, L. A. In "Stereochemistry and Reactivity of Pi Systems"; Watson, W. H., Ed.; Verlag Chemie International: Deerfield Beach, FL, 1983; pp 41–73.
(3) Two earlier reports of note are: (a) Alder, K.; Flock, F. H.; Janssen, P. *Chem. Ber.* **1956**, *89*, 2689. (b) Sugimoto, T.; Kobuke, Y.; Furukawa, J. *J. Org. Chem.* **1976**, *41*, 1457.

(4) The IUPAC name for **1** is tricyclo[5.2.1.0^{2,6}]deca-2,5-diene.
(5) (a) Gleiter, R.; Paquette, L. A. *Acc. Chem. Res.* **1983**, *16*, 328. (b) Gleiter, R.; Böhm, M. C. *Pure Appl. Chem.* **1983**, *55*, 237. (c) Gleiter, R.; Böhm, M. C. In "Stereochemistry and Reactivity of Pi Systems"; Watson, W. H., Ed.; Verlag Chemie International: Deerfield Beach, FL, 1983; pp 105–146. (d) Ginsburg, D. *Tetrahedron* **1983**, *39*, 2095.

Effect of Apical Substitution on Isodicyclopentafulvenes

J. Am. Chem. Soc., Vol. 107, No. 23, 1985 6593

from within the strained norbornyl moiety with the lowest occupied π_s orbital.[5a–c,7] Although the consequences of this interaction in the frontier diene orbital (π_A) are negligible, the subjacent level experiences pronounced tilting at the terminal trigonal carbons in such a way that a disrotatory twist *toward* the apical norbornyl methylene group is present. This analysis of the ground-state properties of **1** is supported by the ^2H and ^{13}C NMR features of substituted derivatives, whose spectra reinforce the notion that electronic influences within the norbornyl segment extend to remarkably long distances.[16]

Isodicyclopentadiene (**1**) can enter into Diels–Alder reactions via four transition states. In the case of Alder approach (maximum overlay of diene and dienophile), steric effects can be expected to dominate and heavily favor above-plane bonding. This pathway is not often followed. When it is, adducts such as **2** are usually
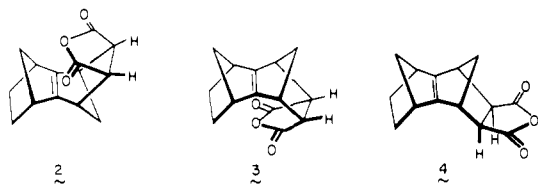
isolated to the exclusion of **3**.[17–19] In those examples where anti-Alder orientations are involved, as they most frequently are in this instance, insignificant steric impediment appears to be offered by the norbornane part of the structure. Nonetheless, the below-plane pathway predominates heavily. One is immediately led to inquire whether the previously described ground-state electronic properties of **1** are responsible for the exceptionally strong penchant for below-plane approach (leading, for example, to **4**).

From the outset, our working hypothesis has been that anti-Alder [4 + 2] cycloadditions to **1** and its congeners are controlled by secondary orbital effects.[2,5] Thus, where **1** is concerned, lesser antibonding interaction between the HOMO of the approaching dienophile and the diene π_s orbital arises during below-plane approach. Above-plane dienophile capture is, however, favored by **5** and related geminal dialkylated derivatives because the

terminal π lobes in these dienes are disrotated *away from* the methano bridge.[16,18a] This contrary deformation can be redressed

through spiroconjugation as in **6**, with return to below-plane π-face stereoselectivity, as the direct consequence of the dominance of σ–π interaction by the diene π_s and cyclopropane Walsh linear combination.[16,18a] These and more recent developments[11,20] have removed from serious consideration the alternative proposal advanced by Vogel[13–15] that the π-facial course of these reactions might be governed by the stability of the isomeric adducts, in line with the Bell–Evans–Polanyi principle. Similarly, Houk's early proposal[21] that the double bonds in **1** might be pyramidalized in an upward direction and thus invite below-plane attack was shown not be contributory by extending the scope of our investigation to include planar fulvenes such as **7**.[22]

Additional support for the existence of product-determinative σ/π interaction in these systems has subsequently been gained from several directions: the highly stereoselective below-plane capture of electrophiles by cyclopentadienide anions such as **8** where analogous orbital tilting is found;[16] the complementary
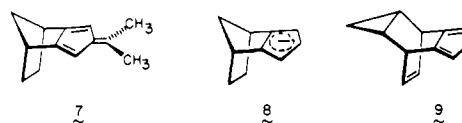
capture of **1** from above-plane during [6 + 4] addition to tropone[1,23] and [3 + 4] addition to oxyallyl cations[23,24] as the result of a substantial increase in the distance between bonding centers in the attacking reagent; the appreciable drop off in π-facial stereoselectivity that accompanies the substitution of vital through-bond interaction[25] with through-space homoconjugation as in **9**;[12] and the strikingly large difference in diastereotopic transition-state energies for [1,5]-sigmatropic hydrogen migration in **1**.[26,27]

Houk's more recent counterproposal consists of attributing full control of the preceding anti-Alder [4 + 2] stereoselectivities to torsional factors, as long as steric effects present in either reactant are not overriding.[28] This interesting hypothesis calls attention to the bending in an endo direction experienced by the incipient norbornene double bond during bottom attack. The resultant flexing is accompanied by a relief of torsional strain involving those bonds attached to the internal cyclopentadiene carbon atoms and the bridgehead C–H bonds greater than that operative during top attack.

A number of our experimental observations appeared inconsistent with this analysis. For example, while diene **10** exhibits no strong predilection for above-plane or below-plane [4 + 2] cycloaddition, the furan analogue **11** enters into Diels-Alder reaction totally by top-face bonding.[25] A stereoselectivity pattern intermediate between those of **1** and **10** has been found for **12**.[20] Although these stereoselectivity trends are consistent with changes in the extent to which superpositioning of the p_y component from

(6) Other structurally related systems that have been examined include tricyclo[5.2.2.0^{2,6}]undeca-2,5,8-triene[7,8] and its perfluorinated derivative,[9] 2,3-norbornenoanthracene,[10] *anti,anti*-2,3-diethylidenenorbornane,[11] tetracyclo[5.3.2.0^{2,6}.0^{8,10}]dodeca-2,5,11-triene,[12] (2-norborneno)[c]furan,[13] various 2-chloromethylene-3-methylene- and 5,6-bis(chloromethylene)bicyclo-[2.2.2]oct-3-enes and 7-oxanorbornanes,[14] and remotely substituted 2,3-dimethylidenebicyclo[2.2.2]octanes.[15]

(7) (a) Paquette, L. A.; Carr, R. V. C.; Böhm, M. C.; Gleiter, R. *J. Am. Chem. Soc.* **1980**, *102*, 1186. (b) Böhm, M. C.; Carr, R. V. C.; Gleiter, R.; Paquette, L. A. *Ibid.* **1980**, *102*, 7218.

(8) Paquette, L. A.; Carr, R. V. C.; Charumilind, P.; Blount, J. F. *J. Org. Chem.* **1980**, *45*, 4922.

(9) (a) Feast, W. J.; Musgrave, W. K. R.; Preston, W. F. *J. Chem. Soc., Perkin Trans. 1* **1972**, 1830. (b) Feast, W. J.; Hughes, R. R.; Musgrave, W. K. R. *Ibid.* **1977**, 152.

(10) Hayes, P. C.; Paquette, L. A. *J. Org. Chem.* **1983**, *48*, 1257.

(11) Paquette, L. A.; Schaefer, A. G.; Blount, J. F. *J. Am. Chem. Soc.* **1983**, *105*, 3642.

(12) Charumilind, P.; Paquette, L. A. *J. Am. Chem. Soc.* **1984**, *106*, 8225.

(13) (a) Avenati, M.; Hagenbuch, J. P.; Mahaim, C.; Vogel, P. *Tetrahedron Lett.* **1980**, 3167. (b) Hagenbuch, J. P.; Vogel, P.; Pinkerton, A. A.; Schwarzenbach, D. *Helv. Chim. Acta* **1981**, *64*, 1818.

(14) (a) Mahaim, C.; Vogel, P. *Helv. Chim. Acta* **1982**, *65*, 866. (b) Avenati, M.; Vogel, P. *Ibid.* **1982**, *65*, 204.

(15) Avenati, M.; Pilet, O.; Carrupt, P.-A.; Vogel, P. *Helv. Chim. Acta* **1982**, *65*, 178.
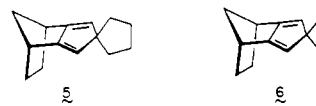
(16) (a) Paquette, L. A.; Charumilind, P. *J. Am. Chem. Soc.* **1982**, *104*, 3749. (b) Paquette, L. A.; Charumilind, P.; Kravetz, T. M.; Böhm, M. C.; Gleiter, R. *Ibid.* **1983**, *105*, 3126.

(17) (a) Watson, W. H.; Galloy, J.; Bartlett, P. D.; Roof, A. A. M. *J. Am. Chem. Soc.* **1981**, *103*, 2022. (b) Bartlett, P. D.; Wu, C. *J. Org. Chem.* **1984**, *49*, 1880.

(18) (a) Paquette, L. A.; Charumilind, P.; Böhm, M. C.; Gleiter, R.; Bass, L. S.; Clardy, J. *J. Am. Chem. Soc.* **1983**, *105*, 3136. (b) Paquette, L. A.; Hayes, P. C.; Charumilind, P.; Böhm, M. C.; Gleiter, R.; Blount, J. F. *Ibid.* **1983**, *105*, 3148.

(19) Ermer, O.; Bodecker, C.-D. *Helv. Chim. Acta* **1983**, *66*, 943.

(20) Paquette, L. A.; Kravetz, T. M.; Hsu, L.-Y. *J. Am. Chem. Soc.*, following paper in this issue.

(21) Rondan, N. G.; Paddon-Row, M. N.; Caramella, P.; Houk, K. N. *J. Am. Chem. Soc.* **1981**, *103*, 2436.

(22) Paquette, L. A.; Kravetz, T. M.; Böhm, M. C.; Gleiter, R. *J. Org. Chem.* **1983**, *48*, 1250.

(23) (a) Paquette, L. A.; Hathaway, S. J.; Kravetz, T. M.; Hsu, L.-Y. *J. Am. Chem. Soc.* **1984**, *106*, 5741. (b) Paquette, L. A.; Hsu, L.-Y.; Gallucci, J. C.; Korp, J. D.; Bernal, I.; Kravetz, T. M.; Hathaway, S. J. *Ibid.* **1984**, *106*, 5743.
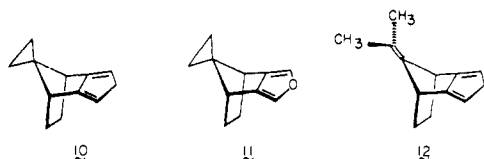
(24) Paquette, L. A.; Kravetz, T. M., unpublished results.

(25) Paquette, L. A.; Green, K. E.; Gleiter, R.; Schafer, W.; Gallucci, J. C. *J. Am. Chem. Soc.* **1984**, *106*, 8232.

(26) Washburn, W. N.; Hillson, R. A. *J. Am. Chem. Soc.* **1984**, *106*, 4575.

(27) Bartlett, P. D.; Wu, C. *J. Am. Chem. Soc.* **1983**, *105*, 100.

(28) Brown, F. K.; Houk, K. N. *J. Am. Chem. Soc.* **1985**, *107*, 1971.

the norbornyl σ frame and the p$_z$ component from the π network occurs,[25] molecular models suggested that those modifications of the apical center in 10–12 exerted little change in the dihedral angle adopted by the bridgehead C–H bonds. Clearly, more definitive structural data were needed to resolve this pivotal question.

In this paper, we describe detailed three-dimensional X-ray studies of three crystalline derivatives of 1, 10, and 12. The isodicyclopentafulvenes 13–15 were selected principally because of advantageous crystallinity properties not shared by the simpler cyclopentadienes. The combined crystal structure results to be
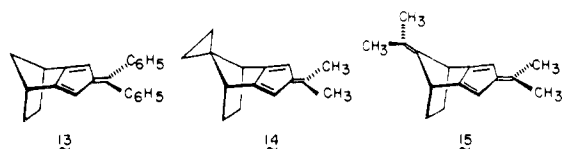

disclosed reveal that little, if any, bridgehead angle deformation accompanies the obviously substantial alteration in hybridization at the apical centers in the three hydrocarbons. As a consequence, the suggestion that torsional effects control stereoselection in these systems is not supported by experimental reality.

Results

Synthesis of the Isodicyclopentafulvenes. Treatment of *tert*-butyl alcohol solutions of the appropriate isodicyclopentadiene and ketone with potassium *tert*-butoxide gave the desired fulvenes in fair to moderate yield. Diphenyl derivative 13 was substituted for the known dimethyl derivative 7 when it was recognized that the latter could not be induced to crystallize suitably. X-ray quality samples of 13–15 were obtained by slow crystallization from ethanol or methanol.

Condensation of 13 with the prototypical dienophile *N*-phenylmaleimide proved sluggish at 70 °C; 1 week in refluxing to toluene was required to consume ca. 50% of the fulvene. The reaction, monitored by ^{1}H NMR and TLC, resulted in formation of a major adduct (84% isolated) identified as 16a on the basis of its ^{1}H NMR spectrum and conversion to epoxide 18a. The
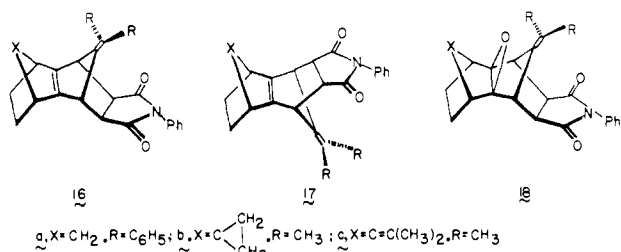
lack of coupling between its bridgehead protons and those at the succinimidyl ring fusion shows the substance to have exo stereochemistry.[29] Its *syn*-sesquinorbornyl nature was confirmed by ^{13}C NMR comparison with 18a. In the epoxide, both apical carbons are more shielded, C9 by 12.19 ppm and C10 by 11.99 ppm. Additionally, olefinic carbon C11 in 18a experiences a downfield shift of 4.94 ppm, in line with expectations arising from the anisotropy contributions of the proximal oxirane ring.[20,22,30]

Figure 1. Numbering scheme for the core atoms common to structures 13, 14, and 15. The letters designate planes of interest in the core.

Figure 2. Drawing for molecule 13 with the numbering scheme for the atoms peripheral to the core. Non-hydrogen atoms are drawn with 50% probability thermal ellipsoids, while hydrogen atoms are drawn with an artificial radius.

A minor adduct (3%) was seen to possess endo stereochemistry (^{1}H NMR) and was therefore formulated as 19 without further characterization.
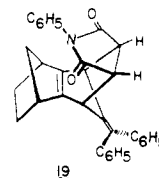
Heating 14 with *N*-phenylmaleimide in benzene solution for 10 h afforded 16b. However, because of the very low scale of this reaction, a minor adduct could have escaped spectroscopic detection.

Comparable treatment of 15 gave rise to a mixture of 16c (56%) and 17c (40%). Stereochemical assignment was again based on ^{1}H NMR analysis, below-plane adduct 16c featuring endo ethano protons at higher field (δ 0.91) than those in 17c (δ 1.16). This ordering is consistent with that observed in many related compounds.[20,25] Imide 17c was noted to undergo retrograde Diels–Alder fragmentation in CDCl$_3$ solution. After 2 days at room temperature, 10% conversion to 16c was realized following thin-layer chromatography on silica gel.

X-ray Diffraction Studies. Space group and unit cell constants were determined for each structure by preliminary examination of the crystals on a Syntex PĪ diffractometer. Unit cell parameters were determined by a least-squares fit of the diffractometer setting angles for at least 19 reflections with $18° < 2\theta < 28°$ using Mo Kα radiation (λ = 0.710 69 Å, graphite monochromator). Intensities were measured at 21 °C by the $\theta - 2\theta$ scan technique with Mo Kα radiation. During the course of the data collection, six standard reflections were measured after every 100 reflections. A decay problem was evident for crystals of 14 and 15; at the end of data collection, the standard reflections measured approximately 65% and 82%, respectively, of their original intensities for 14 and 15. Each data set was corrected for Lorentz and polarization effects and for the observed decay (in the case of 14 and 15) and was put on an approximately absolute scale by means of a Wilson plot.[31] No corrections were made for absorption.

(29) (a) Marchand, A. P.; Rose, J. E. *J. Am. Chem. Soc.* **1968**, *90*, 3724. (b) Marchand, A. P. "Stereochemical Applications of NMR Studies in Rigid Bicyclic Systems"; Verlag Chemie International: Deerfield Beach, FL, 1982.

(30) (a) Paquette, L. A.; Fristad, W. E.; Schuman, C. A.; Beno, M. A.; Christoph, G. G. *J. Am. Chem. Soc.* **1979**, *101*, 4645. (b) Paquette, L. A.; Carr, R. V. C.; Arnold, E.; Clardy, J. *J. Org. Chem.* **1980**, *45*, 4907 and pertinent references cited in these papers.
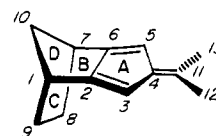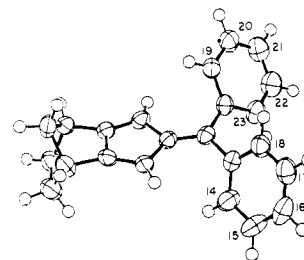
(31) The programs used for data reduction are from the CRYM Crystallographic Computing System (Duchamp, D. J.; Trus, B. L.; Westphal, B. J.), California Institute of Technology, Pasadena, CA, 1964, and modified by G. G. Christoph at The Ohio State University, Columbus, OH. Integrated intensities are calculated as $I = R(C - T(B_1 + B_2))$ where R is the variable scan rate, C is the total scan count, B_1 and B_2 are the background counts, and T is the ratio of the scan time to the total background counting time. The standard deviations are calculated as $\sigma^2(I) = R^2(C + T^2(B_1 + B_2)) + (pI)^2$, where the terms are the same as those defined above, with a value of 0.02 used for p to account for that part of the standard deviation proportional to the diffracted intensity.

Table I. Crystallographic Data for Isodicyclopentafulvenes **13**, **14**, and **15**

	13	14	15
formula	$C_{23}H_{20}$	$C_{15}H_{18}$	$C_{16}H_{20}$
form wt, amu	296.42	198.31	212.34
space group	$P2_1/n$	$P\bar{1}$	$P\bar{1}$
a, Å	9.666 (5)	9.345 (2)	8.078 (1)
b, Å	17.087 (7)	10.502 (2)	6.341 (1)
c, Å	11.229 (6)	5.953 (2)	14.003 (2)
α, deg		91.04 (1)	89.38 (1)
β, deg	116.53 (4)	95.46 (1)	73.45 (1)
γ, deg		84.03 (1)	110.81 (1)
vol, Å³	1659	578	638
Z	4	2	2
ρ_c, g/cm³	1.19	1.14	1.11
cryst dimensions, mm	0.13 × 0.30 × 0.31	0.13 × 0.36 × 0.44	0.06 × 0.26 × 0.46
scan speed, deg/min in 2θ	2.0–24.0	2.0–24.0	2.0–24.0
2θ limits	$4° \leq 2\theta \leq 45°$	$4° \leq 2\theta \leq 55°$	$4° \leq 2\theta \leq 50°$
scan range	$K\alpha_1 -1.0°$ to $K\alpha_2 +1.0°$	$K\alpha_1 -1.0°$ to $K\alpha_2 +1.1°$	$K\alpha_1 -1.0°$ to $K\alpha_2 +1.0°$
background time/scan time	0.5	0.5	0.5
data collected	$+h,+k,\pm l$	$+h,\pm k,\pm l$	$+h,\pm k,\pm l$
unique data	2181	2673	2259
unique data used in refinements	1671	1974	1791
$R^a(F)$	0.070	0.066	0.088
$R_w(F)$	0.047	0.049	0.049
error in observation of unit wt, e	1.55	1.93	1.51

$^a R = \sum ||F_o| - |F_c||/\sum|F_o|$; $R_w = [\sum w(|F_o| - |F_c|)^2/\sum wF_o^2]^{1/2}$.

Figure 3. Diagram for molecule **14** with the numbering scheme for the atoms peripheral to the core. Non-hydrogen atoms are drawn with 50% probability thermal ellipsoids, while hydrogen atoms are drawn with an artificial radius.
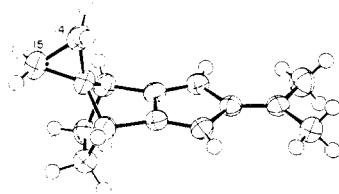

Figure 4. Diagram for molecule **15** with the numbering scheme for the atoms peripheral to the core. Non-hydrogen atoms are drawn with 50% probability thermal ellipsoids, while hydrogen atoms are drawn with an artificial radius.
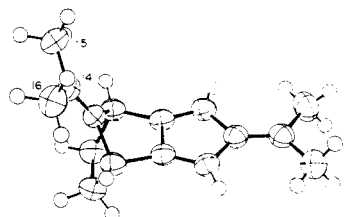
All three structures were solved by direct methods by using MULTAN 80.[32] The SHELX-76 package[33] was used for all full-matrix least-squares refinements; the function $\sum w(|F_o| - |F_c|)^2$ was minimized, where $w = 1/\sigma^2(F_o)$. Scattering factors for the carbon atom[34a] and for the hydrogen atom[34b] are from the usual sources. Crystallographic details for these compounds appear in Table I, and descriptions of the individual refinements appear in the supplementary material along with tables of final positional and thermal parameters for structures **13**, **14**, and **15**.

To facilitate a comparison of the geometries of **13–15**, the core atoms common to all three structures are numbered as shown in Figure 1. Labeling of the atoms peripheral to the core is shown in the drawings for molecules **13**, **14**, and **15** in Figures 2, 3, and

(32) Main, P.; Fiske, S. J.; Hull, S. E.; Lessinger, L.; Germain, G.; Declercq, J.-P.; Woolfson, M. M. "MULTAN 80. A System of Computer Programs for the Automatic Solution of Crystal Structures from X-ray Diffraction Data"; University of York and Louvain: England, and Belgium, 1980.

(33) Sheldrick, G. M. "SHELX-76. Program for Crystal Structure Determination"; University Chemical Laboratory: Cambridge, England, 1976.

(34) (a) "International Tables for X-ray Crystallography"; The Kynoch Press: Birmingham, England, 1974; Vol. IV. (b) Stewart, R. F.; Davidson, E. R.; Simpson, W. T. *J. Chem. Phys.* **1965**, *42*, 3175.

Table II. Bond Distances (Å) for **13**, **14**, and **15**

	13	14	15
	A. Common Bonds		
C1–C2	1.522 (5)^a	1.504 (3)	1.504 (3)
C6–C7	1.495 (4)	1.496 (3)	1.502 (3)
C1–C9	1.533 (5)	1.547 (3)	1.546 (4)
C7–C8	1.538 (4)	1.546 (3)	1.544 (3)
C1–C10	1.554 (4)	1.529 (3)	1.526 (3)
C7–C10	1.540 (5)	1.530 (3)	1.528 (3)
C2–C6	1.467 (4)	1.459 (2)	1.458 (3)
C8–C9	1.544 (4)	1.542 (3)	1.549 (3)
C2–C3	1.339 (4)	1.336 (3)	1.335 (3)
C5–C6	1.324 (4)	1.340 (3)	1.336 (3)
C3–C4	1.469 (4)	1.476 (3)	1.473 (3)
C4–C5	1.483 (4)	1.471 (3)	1.473 (3)
C4–C11	1.345 (4)	1.345 (2)	1.334 (3)
C11–C12	1.484 (4)	1.485 (3)	1.491 (4)
C11–C13	1.475 (4)	1.489 (3)	1.499 (4)
C1–HC1	1.02 (3)	0.97 (2)	0.94 (2)
C7–HC7	0.97 (3)	0.96 (2)	1.00 (2)
	B. Other Bonds		
C12–C14	1.385 (4)		
C14–C15	1.391 (4)		
C15–C16	1.372 (5)		
C16–C17	1.367 (5)		
C17–C18	1.380 (4)		
C18–C12	1.394 (4)		
C13–C19	1.400 (4)		
C19–C20	1.372 (4)		
C20–C21	1.373 (5)		
C21–C22	1.374 (5)		
C22–C23	1.378 (5)		
C23–C13	1.388 (4)		
C10–C14		1.483 (3)	1.311 (3)
C10–C15		1.488 (3)	
C14–C15		1.513 (3)	1.500 (4)
C14–C16			1.498 (4)

^{a} Estimated standard deviations in the least significant figure(s) are given in parentheses in this and all subsequent tables.

4, respectively. Table II contains a list of bond lengths, while Table III contains bond angles for this series. Unit cell drawings illustrating the packing for **13**, **14**, and **15** are presented in Figures 5, 6, and 7, respectively, in the supplementary material. The three structures in this series may be described in terms of noncrystallographic mirror symmetry, where the mirror plane contains atoms C4, C10, and C11 and bisects bond lengths C2–C6 and C8–C9 of the core molecule. With respect to this mirror plane, chemically equivalent bond lengths and angles agree quite well

Table III. Bond Angles (deg) for **13**, **14**, and **15**

	13	14	15
A. Common Bond Angles			
C2–C1–C9	104.0 (3)	106.9 (2)	106.8 (2)
C6–C7–C8	106.3 (3)	106.5 (2)	106.7 (2)
C2–C1–C10	99.3 (3)	99.2 (2)	98.9 (2)
C6–C7–C10	99.6 (3)	99.2 (2)	98.7 (2)
C9–C1–C10	100.0 (3)	99.8 (2)	100.4 (2)
C8–C7–C10	100.3 (3)	100.0 (2)	100.4 (2)
C1–C10–C7	96.2 (3)	96.6 (2)	96.7 (2)
C1–C2–C6	106.3 (3)	105.7 (2)	105.6 (2)
C7–C6–C2	105.8 (3)	106.2 (2)	106.3 (2)
C1–C9–C8	104.4 (3)	103.8 (2)	103.7 (2)
C7–C8–C9	104.2 (3)	104.0 (2)	103.8 (2)
C3–C2–C6	108.8 (3)	109.7 (2)	109.9 (2)
C5–C6–C2	110.2 (3)	109.4 (2)	109.4 (2)
C1–C2–C3	144.7 (3)	144.6 (2)	144.5 (2)
C7–C6–C5	144.0 (3)	144.3 (2)	144.3 (2)
C2–C3–C4	107.8 (3)	107.4 (2)	107.1 (2)
C6–C5–C4	107.3 (3)	107.4 (2)	107.4 (2)
C3–C4–C11	127.4 (3)	126.6 (2)	127.0 (2)
C5–C4–C11	126.7 (3)	127.3 (2)	126.8 (2)
C3–C4–C5	105.8 (3)	106.1 (2)	106.2 (2)
C4–C11–C12	121.3 (3)	123.0 (2)	123.4 (3)
C4–C11–C13	122.0 (3)	122.6 (2)	122.9 (3)
C12–C11–C13	116.6 (3)	114.4 (2)	113.7 (3)
B. Angles Not in Common			
C11–C12–C14	121.3 (3)		
C11–C12–C18	120.4 (3)		
C14–C12–C18	118.3 (3)		
C12–C14–C15	120.6 (4)		
C14–C15–C16	119.7 (4)		
C15–C16–C17	120.7 (4)		
C16–C17–C18	119.8 (4)		
C17–C18–C12	120.9 (4)		
C11–C13–C19	121.4 (3)		
C11–C13–C23	121.2 (3)		
C19–C13–C23	117.4 (3)		
C13–C19–C20	121.2 (4)		
C19–C20–C21	120.5 (4)		
C20–C21–C22	119.2 (4)		
C21–C22–C23	120.8 (4)		
C22–C23–C13	120.8 (3)		
C1–C10–C14		125.0 (2)	131.5 (2)
C1–C10–C15		124.0 (2)	
C7–C10–C14		125.9 (2)	131.8 (2)
C7–C10–C15		124.7 (2)	
C14–C10–C15		61.2 (1)	
C10–C14–C15		59.5 (1)	122.7 (3)
C10–C15–C14		59.2 (1)	
C10–C14–C16			122.5 (3)
C15–C14–C16			114.8 (3)
C. Bond Angles Involving Hydrogen Atoms			
HC1–C1–C2	116.9 (18)	117.1 (10)	117.1 (12)
HC7–C7–C6	115.4 (19)	115.6 (10)	116.1 (11)
HC1–C1–C9	117.9 (19)	114.7 (10)	115.1 (13)
HC7–C7–C8	116.4 (19)	115.2 (11)	115.7 (12)
HC1–C1–C10	115.9 (18)	116.8 (10)	116.2 (13)
HC7–C7–C10	116.4 (19)	118.0 (10)	116.9 (12)

for structure **14** and for structure **15**. The agreement for structure **13** is not as good but is within the limits of error; for example, the worst agreement is between bond lengths C1–C2 and C6–C7, 1.522 and 1.495 Å, respectively, which differ by about five standard deviations. This poorer agreement may be the result of the data set for this structure being the weakest of the three. A comparison of analogous bond lengths and angles between **14** and **15** indicates that the core geometries of these molecules are not significantly different. If molecule **13** is included in this comparison, one finds that the norbornane portion of the core molecule does not agree well with the norbornane portions of **14** and **15**. In **13**, the C1–C10 and C7–C10 bond lengths are longer than the same set of bond lengths in **14** and **15**. The C1–C9 and C7–C8 set is shorter than these sets in **14** and **15**, and the C1–C2 bond length, but not the C6–C7 bond length, is longer than either the C1–C2 or C6–C7 bonds in **14** and **15**.

**Table IV.** Selected Torsion Angles (deg) for **13**, **14**, and **15**

	13	14	15
C3–C4–C11–C12	12.3 (5)	0.3 (3)	–1.7 (6)
C5–C4–C11–C13	9.4 (5)	0.1 (3)	–0.8 (6)
C9–C1–C2–C3	–112.6 (5)	–110.4 (3)	–112.6 (5)
C8–C7–C6–C5	114.2 (5)	110.0 (3)	111.5 (5)
C10–C1–C2–C3	144.6 (5)	146.3 (3)	143.6 (5)
C10–C7–C6–C5	–142.0 (5)	–146.6 (3)	–144.9 (5)
HC1–C1–C2–C3	19.2 (20)	19.8 (12)	18.1 (17)
HC7–C7–C6–C5	–16.4 (21)	–19.4 (11)	–19.1 (18)

Table V. Dihedral Angle (deg) between Planes of the Core Molecule

	13	14	15
A–B	176.7 (2)	179.8 (1)	178.6 (2)
B–C	110.7 (2)	112.3 (1)	112.2 (2)
B–D[a]	125.4 (3)	124.9 (2)	124.1 (3)
C–D	123.8 (3)	122.9 (2)	123.7 (2)

[a] Plane D is the three-atom plane containing atoms C1, C7, and C10.

A further comparison of this core structure can be made with two previously reported structures **20** and **21**[35] which contain almost the same core molecule with the one exception of C4 as an sp^3 carbon in these two structures instead of the sp^2 carbon in **13**, **14**, and **15**. The norbornane fragments for these two
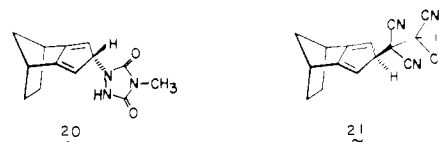
structures do not differ significantly in their bond lengths and angles, and they compare well with the norbornane fragments in molecules **14** and **15** with one exception: the C1–C10 and C7–C10 set of bond lengths is longer (1.543 (5) and 1.550 (6) Å for **20** and 1.542 (4) and 1.540 (4) Å for **21**) than those for **14** and **15**. As the same holds true for structure **13** with respect to **14** and **15**, perhaps this is a result of the lack of substituents on carbon atom C10 in **13**, **20**, and **21**.

As noted for other norbornane derivatives,[36] the value of the angle C1–C10–C7 is markedly different from the tetrahedral value, and the values observed here are almost identical: 96.2°, 96.6°, and 96.7° for **13**, **14**, and **15**, respectively. The angles about the bridgehead carbons also compare favorably in this series. The C9–C1–C10/C8–C7–C10 angle pairs are essentially equal for **13**, **14**, and **15** as are the C2–C1–C10/C6–C7–C10 angle pairs. For the C2–C1–C9/C6–C7–C8 set, it should be noted that the C2–C1–C9 angle for **13** is significantly smaller than the other angles in this set, a phenomenon that may be related to the lengthening of its C1–C2 bond. This agreement among the various bridgehead angles may also be extended to the angles involving hydrogen atoms. The hydrogen atoms bonded to the bridgehead carbons were allowed isotropic refinement for all three structures. Although the hydrogen positions are not nearly as well-determined as the carbon positions in the X-ray experiment, it should be noted that the bond angles involving these hydrogens are not markedly different.

Selected torsion angles are listed in Table IV for **13**, **14**, and **15**. Interestingly, the C4–C11 double bond in **13** is markedly nonplanar with respect to its substituents. The presence of the phenyl groups bonded to C11 may be the cause of this nonplanarity. The dihedral angle between the best least-squares planes through these phenyl rings is 101.1 (1)° and the hydrogen bonded

(35) Paquette, L. A.; Charumilind, P.; Gallucci, J. C. *J. Am. Chem. Soc.* **1983**, *105*, 7364.

(36) (a) Fratini, A. V.; Britts, K.; Karle, I. L. *J. Phys. Chem.* **1967**, *71*, 2482. (b) Macdonald, A. C.; Trotter, J. *Acta Crystallogr.* **1965**, *18*, 243; **1965**, *19*, 456. (c) Filippini, G.; Gramaccioli, C. M.; Rovere, C.; Simonetta, M. *Acta Crystallogr., Sect. B* **1972**, *B28*, 2869. (d) Baker, R.; Wood, J. S. *J. Chem. Soc., Perkin Trans. 2* **1978**, 971. (e) Destro, R.; Filippini, G.; Gramaccioli, C. M.; Simonetta, M. *Acta Crystallogr., Sect. B* **1969**, *B25*, 2465. (f) Craig, R. E. R.; Craig, A. C.; Larsen, R. D.; Caughlan, C. N. *J. Org. Chem.* **1976**, *41*, 2129; **1977**, *42*, 3188.

to C23 of one phenyl ring is pointed inward toward the C12 atom of the second phenyl ring (C12⋯HC23 = 2.79 Å). In **14** and **15**, the C4–C11 double bond is planar. The torsion angles involving the hydrogen atoms bonded to the bridgehead carbons, HC1–C1–C2–C3/HC7–C7–C6–C5, are essentially the same within the limits of error.

The angles between the various least-squares planes of the core molecule as labeled in Figure 1 are presented in Table V. For all three structures, the dihedral angle between planes B and D is slightly larger than the dihedral angle between C and D. A comparison of the dihedral angle between planes A and B for this series shows that for **14**, these two planes are essentially coplanar, while for **15** and **13** these two planes become increasingly non-coplanar.

Conclusions

Since **13**, **14**, and **15** are almost indistinguishable in their overall structural topology, why do they and their simpler isodicyclopentadiene counterparts (**1**, **10**, and **12**) exhibit such varied π-facial stereoselectivity toward dienophiles? The ratios of below-plane vs. above-plane attack show no apparent link to the relative stabilities of the adducts. Thus, when the angles θ at both bridgeheads in *syn*-sesquinorbornene (**22**) are constrained from their normal 115° to 108°, pyramidalization of the internal double bond increases from 14.9° to 15.3°.[37] This effect is seemingly negligible
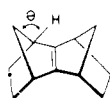
22

since fully optimized **22** is 1.9 kcal/mol more stable than the anti isomer (MM2), while constraint in the predescribed manner increases the difference to only 2.0 kcal/mol.[37]

In our view, possible explanations of the increased tendency of **10**[25] and **12**[20] (relative to **1**) for above-plane [4 + 2] cyclo-addition have now been substantially narrowed. The dihedral angles between the bridgehead C–H bonds in **13** (–16.4°, 19.2°) are not significantly different from those found in **14** (–19.4°, 19.8°) and **15** (–19.1°, 18.1°). Accordingly, torsional effects engendered between these bonds and those involving the cyclo-pentadiene double bonds should not only be closely comparable but unidirectionally favorable to dienophile capture from the same surface. We now recognize this not to be the case, particularly as demonstrated for **1**, **10**, and **12** with dienophiles of widely ranging reactivity.

Since product stabilities calculated by the MM2 procedure continue to favor *syn*-sesquinorbornene geometries in all three instances, the influx of a high percentage of above-plane addition with formation of anti frameworks, in particular with **10** and **12**, defies explanation in these terms.

On the other hand, this modulation of stereoselectivity can be satisfactorily accommodated within the guidelines of the Paquette–Gleiter hypothesis.[2,5a–c] As detailed in the accompanying paper,[20] the observed reduction in below-plane addition that accompanies the grafting of a spirocyclopropane ring or iso-propylidene group onto the methano bridge leads to a reduction in π-orbital tilting within π₁ and a diminished ability to direct capture of the dienophile from below the cyclopentadiene plane.

Experimental Section

2-(Diphenylmethylene)-4,5,6,7-tetrahydro-4,7-methano-2*H*-indene (13). A mixture of **1** (0.30 g, 2.3 mmol), benzophenone (0.41 g, 2.3 mmol), and potassium *tert*-butoxide (0.64 g, 5.7 mmol) in anhydrous *tert*-butyl alcohol (4 mL) was stirred at the reflux temperature for 6 h. The reaction mixture was cooled to 20 °C, diluted with water (5 mL), and extracted with methylene chloride (4 × 5 mL). The combined organic extracts were washed with water, dried, and freed of solvent to yield a bright-orange oil. Purification by preparative thin-layer silica gel chromatography (elution with petroleum ether) provided 381 mg (58%) of **13** as orange needles: mp 120–121 °C (from methanol); IR (CDCl₃,

(37) Houk, K. N., private communication, Jan 8, 1985.

cm⁻¹) 3055, 2970, 2870, 1595, 1490, 1440, 1330, 1100, 830; ¹H NMR (300 MHz, CDCl₃) δ 7.32 (m, 10 H), 5.72 (s, 2 H), 3.09 (m, 2 H), 1.88 (d, *J* = 7.2 Hz, 2 H), 1.79 (d, *J* = 9.1 Hz, 1 H), 1.73 (d, *J* = 9.1 Hz, 1 H), 1.47 (dd, *J* = 7.2 and 1.8 Hz, 2 H); ¹³C NMR (20 MHz, CDCl₃) δ 157.31, 149.21, 146.10, 142.11, 131.56, 127.67, 127.56, 108.43, 45.06, 38.83, 28.94; MS, *m/z* (M⁺) calcd 296.1565, obsd 296.1576.

Anal. Calcd for C₂₃H₂₀: C, 93.20; H, 6.80. Found: C, 93.04; H, 6.91.

4′,5′,6′,7′-Tetrahydro-2′-isopropylidenespiro[cyclopropa-1,2′-[4,7]-methano[2*H*]indene] (14). To a solution of anhydrous *tert*-butyl alcohol (1.5 mL) containing freshly cut potassium (62 mg, 1.6 mmol) was added **10** (100 mg, 0.63 mmol) dissolved in acetone (1 mL). After 10 h of stirring, the yellow solution turned red. Water was added, and the product was extracted into dichloromethane. The organic layer was washed with brine, dried, and evaporated to leave a residue which was purified by preparative TLC chromatography (silica gel, elution with 3% ethyl acetate in petroleum ether). There was isolated 17.2 mg (13.7%) of **14** as a yellow crystalline solid: mp 96–97 °C (from methanol); ¹H NMR (300 MHz, CDCl₃) δ 5.96 (s, 2 H), 2.33–2.32 (m, 2 H), 2.11 (s, 6 H), 1.57 (br s, 2 H), 1.49 (dd, *J* = 12.5 and 5.5 Hz, 2 H), 0.53–0.50 (m, 4 H); ¹³C NMR (80 MHz, CDCl₃) δ 155.74, 146.22, 142.96, 105.24, 44.72, 41.30, 29.07, 22.74, 6.37, 6.02; MS, *m/z* (M⁺) calcd 198.1408, obsd 198.1402.

4,5,6,7-Tetrahydro-2,8-diisopropylidene-4,7-methano-2*H*-indene (15). Triene **12** (70 mg, 0.41 mmol) was added to a freshly prepared solution of sodium methoxide (23 mg, 1.0 mmol of sodium) in anhydrous methanol (2 mL) at 40 °C and was stirred for 15 min. Acetone (50 mg, 0.86 mmol) was added, and the mixture was stirred at the same temperature for 18 h. After cooling to 20 °C, the mixture was diluted with petroleum ether (5 mL) and washed with water until neutral. The organic solution was dried, filtered, and evaporated to give a yellow oil which, after preparative thin-layer silica gel chromatography (elution with petroleum ether), afforded 10 mg (15% based on recovered triene) of **15** as yellow needles: mp 113–115 °C (from ethanol); IR (KBr, cm⁻¹) 2998, 2965, 2930, 2865, 1655, 1440, 1370, 1338, 810; ¹H NMR (300 MHz, C₆D₆) δ 6.10 (s, 2 H), 3.63 (m, 2 H), 1.90 (s, 6 H), 1.88 (m, 2 H), 1.64–1.59 (m, 2 H), 1.62 (s, 6 H); ¹³C NMR (20 MHz, CDCl₃) δ 153.63, 146.11, 143.73, 143.30, 114.10, 104.48, 39.86, 28.81, 22.85, 20.50; MS, *m/z* (M⁺) calcd 212.1565, obsd 212.1563.

***N*-Phenylmaleimide Cycloadditions to the Isodicyclopentafulvenes. A.** A solution of **13** (180 mg, 0.61 mmol) and *N*-phenylmaleimide (158 mg, 0.91 mmol) in toluene (10 mL) was heated at the reflux temperature for 6 days. After cooling to 20 °C, solvent was removed in vacuo, and the resulting oily mixture was separated by medium-pressure liquid chromatography on silica gel (elution with 30% ethyl acetate in petroleum ether) to provide 81 mg (53%) of recovered **13** and two cycloadducts in a combined yield of 87% (based on recovered **13**).

For **16a**: 112 mg (84%) of colorless solid, mp 190–191 °C (from hexanes); IR (CDCl₃, cm⁻¹) 2985, 2890, 1715, 1500, 1445, 1385, 1190; ¹H NMR (300 MHz, CDCl₃) δ 7.48–7.05 (series of m, 15 H), 4.09 (s, 2 H), 3.19 (m, 2 H), 2.87 (s, 2 H), 1.72 (d, *J* = 7.5 Hz, 2 H), 1.50 (d, *J* = 8.1 Hz, 1 H), 1.16 (d, *J* = 8.2 Hz, 1 H), 0.93–0.90 (m, 2 H); ¹³C NMR (20 MHz, CDCl₃) δ 176.12 (s), 153.31 (s), 145.65 (s), 140.47 (s), 131.27 (s), 129.29 (d), 128.72 (s), 128.21 (d), 127.12 (d), 126.67 (d), 49.70 (t), 49.06 (d), 48.36 (d), 43.37 (d); 25.42 (m); MS, *m/z* (M⁺) calcd 469.2042, obsd 469.2022.

Anal. Calcd for C₃₃H₂₇NO₂: C, 84.41; H, 5.80. Found: C, 84.02; H, 6.16.

For **19**: 3 mg (3%) of colorless solid, mp 131–132 °C (from ethyl acetate); ¹H NMR (300 MHz, CDCl₃) δ 7.41–6.99 (series of m, 15 H), 3.98 (m, 2 H), 3.67 (m, 2 H), 3.10 (m, 2 H), 1.76–1.71 (m, 2 H), 1.26–1.11 (series of m, 4 H); MS, *m/z* (M⁺) calcd 469.2042, obsd 469.2042.

B. A 3-mg sample of **14** was heated with ca. 1 mol equiv of *N*-phenylmaleimide in benzene at the reflux temperature for 10 h. The solvent was evaporated to leave a solid whose 300-MHz ¹H NMR spectrum in CDCl₃ was uniquely compatible with formulation as **16b**: ¹H NMR (300 MHz) δ 7.48–7.05 (series of m, 5 H), 4.02 (s, 2 H), 2.82 (s, 2 H), 2.45 (s, 2 H), 1.85 (d, *J* = 8.2 Hz, 2 H), 1.60 (s, 6 H), 0.98 (m, 2 H), 0.55 (m, 2 H), 0.34 (m, 2 H); MS, *m/z* (M⁺) calcd 371.1884, obsd 371.1884.

C. A solution of **15** (40 mg, 0.19 mmol) and *N*-phenylmaleimide (39 mg, 0.23 mmol) in deoxygenated benzene (0.5 mL) stood at 20 °C for 3 days. Solvent was removed in vacuo, and the residue was subjected to medium-pressure liquid chromatography on silica gel (elution with 12% ethyl acetate in petroleum ether). Two cycloadducts were isolated in a combined yield of 96%.

For **16c**: 41 mg (56%) of colorless needles, mp 185–186 °C (from hexanes); IR (KBr, cm⁻¹) 3000, 2940, 1715, 1500, 1375, 1170; ¹H NMR (300 MHz, CDCl₃) δ 7.48–7.37 (m, 3 H), 7.11–7.09 (m, 2 H), 4.02 (s,

2 H), 3.61 (m, 2 H), 2.80 (s, 2 H), 1.68 (d, J = 7.0 Hz, 2 H), 1.60 (s, 6 H), 1.57 (s, 6 H), 0.91 (dd, J = 11.5 and 4.0 Hz, 2 H); ^{13}C NMR (75 MHz, CDCl$_3$) δ 176.39, 152.36, 146.84, 140.40, 131.88, 129.20, 128.58, 126.30, 115.79, 109.12, 48.44, 47.80, 43.37, 25.42, 20.19, 19.92; MS, m/z (M$^+$) calcd 385.2041, obsd 385.2043.

For **17c**: 29 mg (40%) of colorless needles, mp 139–140 °C (from hexanes); IR (KBr, cm^{-1}) 3000, 2985, 2985, 2930, 2860, 1717, 1500, 1445, 1370, 1190; ^{1}H NMR (300 MHz, CDCl$_3$) δ 7.47–7.36 (m, 3 H), 7.11–7.09 (m, 2 H), 3.91 (s, 2 H), 3.44 (m, 2 H), 2.94 (s, 2 H), 1.74 (d, J = 7.3 Hz, 2 H), 1.54 (s, 6 H), 1.49 (s, 6 H), 1.16 (dd, J = 10.5 and 4.3 Hz, 2 H); ^{13}C NMR (75 MHz, CDCl$_3$) δ 176.61, 155.40, 150.79, 142.86, 132.02, 129.16, 128.55, 126.39, 112.92, 108.70, 49.13, 49.74, 42.19, 25.84, 19.70, 19.40; MS, m/z (M$^+$) calcd 385.2042, obsd 385.2050.

4a,8a-Epoxy-1,2,3,4,4a,5,6,7,8,8a-decahydro-9-(diphenylmethylene)-N-phenyl-syn-(1,4:5,8-dimethano)naphthalene-6,7-dicarboximide (18a). m-Chloroperbenzoic acid (11 mg, 0.064 mmol) was added to a solution of **16a** (30 mg, 0.064 mmol) in methylene chloride (5 mL) at 0 °C, and the mixture was stirred at the same temperature for 3 h and then at –10 °C for 15 h. After warming to 20 °C, the mixture was washed with 5% aqueous sodium bisulfite solution (2 × 5 mL), 10% aqueous sodium bicarbonate solution (1 × 5 mL), and water (until neutral) and then dried, filtered, and evaporated to give a colorless solid. Purification using medium-pressure silica gel chromatography (elution with 20% ethyl acetate in petroleum ether) provided 23 mg (74%) of **18a** as a colorless solid, mp 294–295 °C (from ethyl acetate); IR (KBr, cm^{-1}) 3000, 1720, 1500, 1390, 1190, 700, 690; ^{1}H NMR (300 MHz, CDCl$_3$) δ 7.51–7.07 (series of m, 15 H), 3.94 (s, 2 H), 3.66 (s, 2 H), 2.95 (m, 2 H), 1.92 (d, J = 9.7 Hz, 1 H), 1.76 (m, 4 H), 0.85 (d, J = 9.3 Hz, 1 H); ^{13}C NMR (75 MHz, CDCl$_3$) δ 176.17 (s), 140.47 (s), 136.60 (s), 133.66 (s), 131.64 (s), 129.39 (d), 129.00 (d), 128.89 (d), 128.18 (d), 127.13 (d), 126.48 (d), 57.14 (s), 47.93 (d), 46.88 (d), 40.92 (d), 37.51 (t), 26.60 (m); MS, m/z (M$^+$) calcd 485.1991, obsd 485.2015.

Supplementary Material Available: Crystallographic details, tables of positional and thermal parameters, as well as unit cell drawings for **13**, **14**, and **15** (Tables VI–VIII, Figures 5–7) (10 pages). Ordering information is given on any current masthead page.
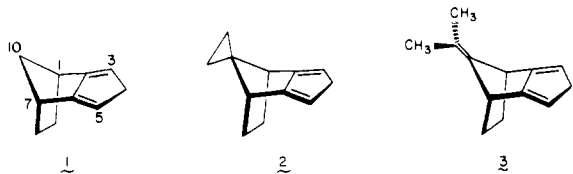
Electronic Control of Stereoselectivity 31. π-Facial Course of Diels–Alder Cycloadditions to 10-Isopropylideneisodicyclopentadiene[1]

Leo A. Paquette,* Tina M. Kravetz, and Leh-Yeh Hsu[2]

Contribution from the Evans Chemical Laboratories, The Ohio State University, Columbus, Ohio 43210. Received April 1, 1985

Abstract: 10-Isopropylideneisodicyclopentadiene (**3**) has been synthesized and its stereoselective behavior during Diels–Alder cycloaddition to N-methyltriazolinedione, dimethyl acetylenedicarboxylate, N-phenylmaleimide, p-benzoquinone, and phenyl vinyl sulfone examined in detail. Structural assignments to the adducts were made on the basis of spectral data, X-ray crystal structure determination, and chemical reactivity, especially sensitivity to triplet oxygen leading to epoxide formation. Less control of π-face selectivity was seen relative to the control exhibited by the parent isodicyclopentadiene. In the case of benzoquinone, the Alder above-plane adduct was observed to be capable of retrograde fragmentation and conversion to two isomeric compounds. A second observation of interest was the isolation of **23**, only the second known example of Alder below-plane bonding in this series. The data are shown to conform plausibly to the Gleiter–Paquette electronic model for these reactions and not to fit satisfactorily the Brown–Houk torsional strain hypothesis.

Although Diels–Alder cycloadditions to isodicyclopentadiene (**1**) have been scrutinized by several groups,[3–6] no general agreement has been reached concerning the origin of the remarkable π-facial stereoselectivities that are encountered.[7–10]

From among the various hypotheses offered to date, two remain as viable proposals worthy of more detailed scrutiny. The first, suggested by Gleiter and Paquette,[5b,8] is founded on the evident strong admixing of the norbornyl σ-orbital framework with the diene π$_s$ orbital. The result is a notable disrotatory tilting within the terminal pπ orbitals toward the methano bridge. The working model invokes direct involvement of these subjacent orbital effects in the control of anti-Alder [4 + 2] cycloaddition, with preferred below-plane capture of the dienophile in order to minimize antibonding interactions. The contrasting Alder arrangement of the reactants seemingly favored by the more reactive dienophiles comes under ordinary steric control and leads to above-plane bonding.[5e]

(1) Part 30. Gallucci, J. C.; Kravetz, T. M.; Green, K. E.; Paquette, L. A. *J. Am. Chem. Soc.*, preceding paper in this issue.
(2) Author to whom queries concerning the X-ray analyses should be directed.
(3) Alder, K.; Flock, F. H.; Janssen, P. *Chem. Ber.* **1956**, *89*, 2689.
(4) Sugimoto, T.; Kobuke, Y.; Furukawa, J. *J. Org. Chem.* **1976**, *41*, 1457.
(5) (a) Paquette, L. A.; Carr, R. V. C.; Böhm, M. C.; Gleiter, R. *J. Am. Chem. Soc.* **1980**, *102*, 1186. (b) Böhm, M. C.; Carr, R. V. C.; Gleiter, R.; Paquette, L. A. *Ibid.* **1980**, *102*, 7218. (c) Paquette, L. A.; Carr, R. V. C.; Arnold, E.; Clardy, J. *J. Org. Chem.* **1980**, *45*, 4907. (d) Paquette, L. A.; Carr, R. V. C.; Charumilind, P.; Blount, J. F. *Ibid.* **1980**, *45*, 4922. (e) Paquette, L. A.; Green, K. E.; Hsu, L.-Y. *Ibid.* **1984**, *49*, 3650.
(6) (a) Watson, W. H.; Galloy, J.; Bartlett, P. D.; Roof, A. A. M. *J. Am. Chem. Soc.* **1981**, *103*, 2022. (b) Bartlett, P. D.; Wu, C. *J. Org. Chem.* **1984**, *49*, 1880.

(7) (a) Avenati, M.; Hagenbuch, J. P.; Mahaim, C.; Vogel, P. *Tetrahedron Lett.* **1980**, 3167. (b) Hagenbuch, J. P.; Vogel, P.; Pinkerton, A. A.; Schwarzenbach, D. *Helv. Chim. Acta* **1981**, *64*, 1818. (c) Mahaim, C.; Vogel, P. *Ibid.* **1982**, *65*, 204, 866. (d) Avenati, M.; Pilet, O.; Carrupt, P.-A.; Vogel, P. *Ibid.* **1982**, *65*, 178.
(8) (a) Gleiter, R.; Paquette, L. A. *Acc. Chem. Res.* **1983**, *61*, 328. (b) Paquette, L. A. In "Stereochemistry and Reactivity of Pi Systems"; Watson, W. H., Ed.; Verlag Chemie International: Deerfield Beach, FL, 1983; pp 41–73. (c) Gleiter, R.; Böhm, M. C. *Ibid.*, pp 105–146. (d) Gleiter, R.; Böhm, M. C. *Pure Appl. Chem.* **1983**, *55*, 237.
(9) Rondan, N. G.; Paddon-Row, M. N.; Caramella, P.; Houk, K. N. *J. Am. Chem. Soc.* **1981**, *103*, 2436.
(10) Brown, F. K.; Houk, K. N. *J. Am. Chem. Soc.* **1985**, *107*, 1971.